Cent. Eur. J. Chem. • 7(3) • 2009 • 555-559
DOI: 10.2478/s11532-009-0049-4

VERSITA

Central European Journal of **Chemistry**

A green chemical route for the synthesis of Mn_3O_4 nanoparticles

Research Article

Zehra Durmus[a], Hüseyin Kavas[b], Abdulhadi Baykal[a*], Muhammet S. Toprak[c]

[a]Department of Chemistry,
Fatih University,
34500 Istanbul, Turkey

[b]Department of Physics,
Fatih University,
34500 Istanbul, Turkey

[c]Functional Materials Division,
Royal Institute of Technology,
SE16440 Stockholm, Sweden

Received 02 January 2009; Accepted 02 March 2009

Abstract: A novel environmental friendly, room temperature route using an ionic liquid 1-n-butyl-3-methylimidazolium hydroxide ([BMIM]OH) for the synthesis of Mn_3O_4 nanoparticles is presented. The product was characterized using Fourier transform infrared spectroscopy, X-ray powder diffraction, and transmission electron microscopy. Phase purity was confirmed by XRD, and X-ray line profile fitting determined a crystallite size of 42 ± 11 nm. TEM analysis revealed various morphologies. EPR measurements have indicated the existence of long-range interactions, due to the wide range of particle sizes and morphologies observed .

Keywords: *Ionic liquids • Nanoparticles •* Mn_3O_4 *• [BMIM]OH • TEM • EPR*

1. Introduction

Transition-metal oxide nanoparticles can exhibit enhanced optical, magnetic and electrical properties as compared to their bulk counterparts, rendering such nanoparticles interesting for a variety of applications [1,2]. Among magnetic nanoparticles, manganese oxide (Mn_3O_4) as a magnetic transition metal oxide is an important material. It has a wide range of applications as catalyst, ion-exchange medium, molecular adsorbent, and in electrochemical materials and varistors [3-7]. Furthermore, Mn_3O_4 has been widely used as the main source of ferrite materials, finding extensive applications in electronics and information technologies. Mn_3O_4 is known to crystallize in the normal spinel structure with a tetragonal distortion elongated along the c-axis. Manganese ions are placed in the tetrahedral A-sites (Mn^{2+}) and octahedral B-sites (Mn^{3+}). A variety of methods including high temperature sol–gel [8], sonochemical [9], co-precipitation [10], solvothermal [11], hydrothermal [12], chemical bath deposition [13], oxidation [14,15], microwave irradiation [16] and surfactant-assisted methods [17] have been reported for its synthesis.

Most recently, the synthesis of nano- and microstructured inorganic materials at room temperature in ionic liquids (ILs) has attracted increasing attention because of increasing consciousness in the context of green synthesis as an environment-friendly and economic alternative to the traditional routes, which use toxic organic solvents [18]. ILs are organic salts with low melting temperature (< 100°C), composed of ions, and exhibiting high thermal stability. These liquids have interesting chemical and physical properties including large electrochemical window, high chemical and thermal stability, non-volatility, controlled miscibility, non-flammability, negligible vapor pressure, and

---

* *E-mail: hbaykal@fatih.edu.tr*

good electrical stability for separations [19,20] and electrochemistry [21]. Ionic liquids can act as solvents for reactants and as morphology templates for the products at the same time, which enables the synthesis of inorganic materials with improved properties [22]. Although ILs are promising solvents for inorganic material synthesis, very few studies have reported the use of these materials for the synthesis of metal oxides [22-25].

In this work we present a room temperature, green chemical route for the fabrication of Mn_3O_4 nanocrystals which is, to the best of our knowledge, the first report of the synthesis of Mn_3O_4 nanocrystals in ionic liquid media at room temperature.

2. Experimental Procedures

2.1. Synthesis of Mn_3O_4 nanoparticles at presence of ionic liquid

All chemicals were analytical grade and were used without further purification. Ionic liquid 1-n-butyl-3-methylimidazolium hydroxide, [BMIM]OH, was prepared according to [26]. In a typical procedure $Mn(NO_3)_2 \times 4H_2O$ was added to 2.0 g of [BMIM]OH at room temperature. Then an aliquot of 2M NaOH solution was added. H_2O_2 (30 w/w %, 5 mL) was added to the mixture drop-wise over a period of 30 min. The brown product was separated by centrifugation, washed with deionized water and then with absolute ethanol, and dried in vacuum overnight.

2.2. Characterization

X-ray powder diffraction (XRD) analysis was conducted on a Huber JSODebyeflex 1001 diffractometer operated at 40 kV and 35 mA using Cu K_α radiation.

Fourier transform infrared (FT-IR) spectra of the samples were recorded with a Perkin Elmer BX FT-IR infrared spectrometer in the range of 4000-400 cm^{-1}.

Transmission electron microscopy (TEM) analysis was performed using a FEI Tecnai G2 Sphera microscope. A drop of diluted sample in alcohol was dripped on the TEM grid and dried before transferring the sample into TEM column for analysis.

A conventional X-band (f = 9.8 GHz) Bruker EMX model EPR spectrometer employing an ac magnetic field (100 kHz) modulation technique was used to record the first derivative absorption signal.

3. Result and Discussion

In this study, syntheses of Mn_3O_4 nanocrystals were performed at room temperature, using an environment friendly ionic liquid [BMIM]OH, which was recovered at the end of the synthesis process. The nanoparticles produced were then characterized using XRD for the identification of the crystalline phases present.

3.1. XRD Analysis

A typical XRD pattern of the synthesized Mn_3O_4 powder is shown in Fig. 1. All diffraction peaks were indexed to tetragonal Mn_3O_4 (ICDD Card no. 24-0734). No extra peaks indicating impurities or other forms of manganese oxides were detected. The average size of the crystallites, D, was estimated from the diffraction pattern using line profile fitting as described in Wejrzanowski *et al*. [27] and Pielaszek [28]. The line profile, shown in Fig. 1, is fitted for 14 peaks with the following Miller indices: (112), (220), (013), (211), (004), (220), (204), (015), (312), (224), (116), (400), (411) and (304). An average crystallite size, D_{XRD}, of 41.5 ± 11 nm was thus obtained for the synthesized Mn_3O_4 nanocrystals.

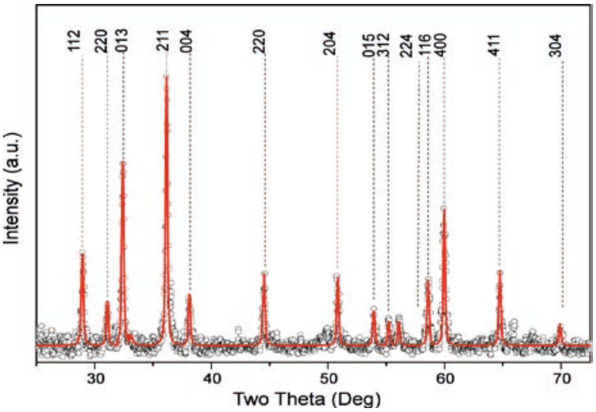

Figure 1. XRD pattern of the Mn_3O_4 nanoparticles and profile fitting.

Zou *et al*. [22] reported on the possible formation mechanism of Co_3O_4 nanoparticles in the presence of ionic liquid at room temperature. They suggested that Ionic liquid acted both as the reaction medium and as an electrical conductor which accelerated electron transfer. The following analogous mechanism is suggested for the formation of Mn_3O_4:

$$Mn^{2+} + 2\,OH^- \rightarrow Mn(OH)_2 \qquad (1)$$

$$3Mn(OH)_2 + H_2O_2 \xrightarrow[25^{\circ}C]{[BMIM]OH} Mn_3O_4 + 4H_2O \qquad (2)$$

Here the key point is the presence of the IL for electron transfer. For the synthesis of Mn_3O_4 nanocrystals in the presence of H_2O_2, the use of IL is therefore crucial.

3.2. FTIR Analysis

FTIR analysis was performed for the prepared sample. The spectrum is presented in Fig. 2. Two broad peaks at 3414 and 1620 cm^{-1} are assigned to O-H stretching and bending modes of adsorbed water. Two absorption bands observed at 625 and 515 cm^{-1}, are associated with the coupling between Mn-O stretching modes of tetrahedral A- and octahedral B- sites [29,30] as expected from normal spinel structure. Thus, the FTIR spectrum further confirms that the product is Mn_3O_4.

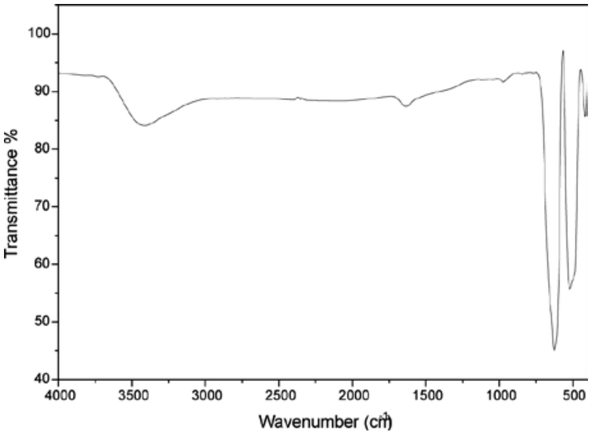

Figure 2. FTIR spectra of as-synthesized Mn_3O_4 nanoparticles.

3.3. TEM Analysis

Morphologies of synthesized Mn_3O_4 nanoparticles were investigated by TEM, and a few micrographs are presented in Fig. 3. A wide dispersion of particle size was detected. A variety of morphologies mainly including spheroid, tetragonal and rod shaped have been observed. Particle size calculations, estimated from the TEM micrographs after counting a minimum of 300 nanoparticles, resulted in the following distribution: 45% spherical nanoparticles with diameters between 58 and 388 nm; 47% cubic particles with size between 85 and 360 nm; and 8% nanorods with aspect ratios in the range of 98 × 360 nm to 104 × 683 nm. A comparison of crystallite size obtained from XRD analysis with the TEM observations reveals the polycrystalline nature of Mn_3O_4 nanoparticles synthesized using ILs.

Experimental facilities did not allow for a constant dropping rate of H_2O_2. This is the most probable cause of the formation of different morphologies. To achieve a single morphology, the dropping rate must be controlled. Chen *et al*. [14] invetigated the effect of dropping rate of H_2O_2 on the formation of Mn_3O_4 nanoparticles.

3.4. EPR Analysis

The magnetic properties of the synthesized Mn_3O_4 were measured using an EPR technique in X band. The spectrum is presented in Fig. 4. EPR analysis gave some facts about the interactions in nano manganese oxide. Broad EPR lines are observed without hyperfine splitting for Mn^{+2} and Mn^{+4} with linewidth of 2787 Gauss and resonance field of 4026 Gauss. This symmetric broad line shows the existence of strongly interacting Mn^{+2} ions in Mn_3O_4 which is the result of convolution of different resonance fields due to the distribution of local effective fields during dipolar interactions between particles as suggested by Winkler *et al*. [31]. Moreover, in our study, the anisotropy resulting from a broad size distribution in the range of 8-680 nm and various morphologies can cause wide range inter-particle and intra-particle interactions. Smaller particles in the product may have magnetically disordered surface comparable with the total volume. These type of structures can be classified as core-shell structures and they include clusters of free spins located at this disordered surface. In our earlier work, we reported on

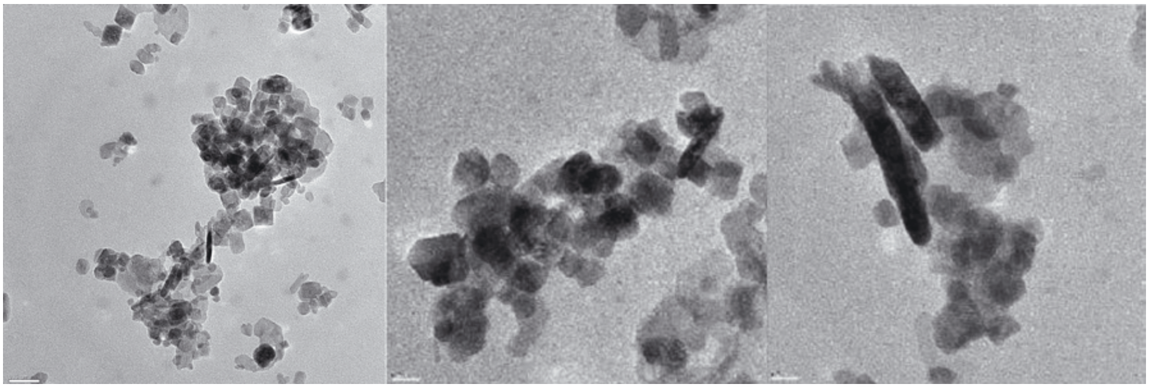

Figure 3. TEM micrographs of as-synthesized Mn_3O_4 nanoparticles with various morphologies (Scale bars are white and located at the left side of each micrographs with 50 nm length).

their effects by vibrating sample magnetometry (VSM) for Mn_3O_4 obtained *via* different methods [10]. And also Alvarez *et al*. [32] synthesized and characterized manganese core-shell nanoparticles with average sizes ranging from 5 to 60 nm. All of the above listed factors may cause broad EPR lines and smaller g values (1.55) than the literature g value for Mn_3O_4 (2.01). This might be due to exchange-coupled systems with unlike spins such as canted spin at particle surfaces, arising from the nature of the core-shell structure.

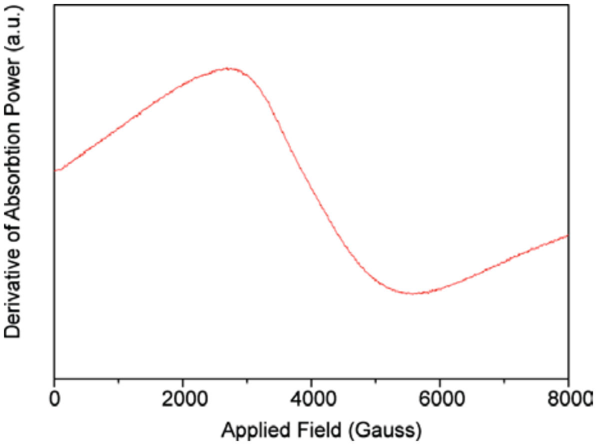

Figure 4. ESR absorption spectrum of Mn_3O_4.

4. Conclusion

Mn_3O_4 nanoparticles have been successfully synthesized by a novel method using an ionic liquid, [BMIM]OH at room temperature. The ionic liquid [BMIM]OH plays an important role in the reaction as the electric conductor medium. This route could be considered as a novel, environmental friendly, and fast method to prepare nanostructured Mn_3O_4 and similar oxide systems. Phase purity was confirmed by XRD and a crystallite size of 45 ± 11 nm was obtained by x-ray line profile fitting. TEM analysis revealed various morphologies and particle sizes which clearly indicates the polycrystalline nature of observed nanoparticles. Long-range interactions as indicated by the EPR measurements might be due to the wide range of particle sizes and morphologies observed.

Acknowledgements

The authors are thankful to the Fatih University Research Project Foundation (Contract no: P50020803-2) and Turkish Ministry of Industry and Trade (Contract no: 00185.STZ.2007-2) for financial support of this study. The fellowship from Knut and Alice Wallenbergs Foundation is also thankfully acknowledged (No:UAW2004.0224) by Dr. M.S.Toprak. The authors also thank to Dr. Brindaban C. Ranu (Indian Association for the Cultivation of Science) for his helpful contributions.

References

[1] Y.F. Shen, et al., Science 260, 511 (1993)
[2] D.K. Kim, et al., J. Appl.Phys. 97, 10J510 (2005)
[3] A.R. Armstrong, et al., Nature 381, 499 (1996)
[4] M.C. Bernard, et al., J. Electrochem. Soc. 140, 3065 (1993)
[5] A.H. De Vries, et al., Phys. Rev. B 66, 35108 (2002)
[6] Y. Yamashita, et al., Surf. Sci. 514, 54 (2002)
[7] J. Li, et al., Appl. Phys. Lett. 70, 3047 (1997)
[8] S. Ching, et al., Chem. Mater. 9, 750 (1997)
[9] A. Askarinejad, A. Morsali, Ultrason. Sonochem. 16, 124 (2009)
[10] T. Ozkaya, et al., Physica B 403, 3760 (2008)
[11] E. Finocchio, G. Busca. Catal. Today 70, 213 (2001)
[12] Z.Y. Chang, et al., J. Solid State Chem. 177, 4093 (2004)
[13] Y.Q. Chang, et al., J. Cryst. Growth 264, 232 (2004)
[14] Z.W. Chen, et al., Scripta Materialia 55, 735 (2006)
[15] J. Moon, et al., MRS 14, 4594 (1999)
[16] A. Baykal, et al., Cent. Eur. J. Chem. 5, 169 (2007)
[17] T. Ozkaya, BSc thesis, Fatih University (İstanbul, Turkey, 2008)
[18] T. Welton, Chem. Rev. 99, 2071 (1999)
[19] G. Drake, et al., Propellants Explosives Pyrotechnics 28, 174 (2003)
[20] J.G. Huddleston, et al., Chem. Commun 16, 1765 (1998)
[21] E.V. Dickinsonet, et al., J. Am. Chem. Soc. 121, 613 (1999)
[22] D. Zou, et al., Materials Letters 62, 1976 (2008)
[23] T. Nakashima, N. Kimizuka, J. Am. Chem. Soc. 125, 6386 (2003)
[24] Y. Zhou, M. Antonietti, Adv. Mater. 15, 1452 (2003)
[25] Y. Zhou, M. Antonietti, J. Am. Chem. Soc. 125, 14960 (2003)

[26] B.C. Ranu, S. Banerjee, Organic Letters 7, 3049 (2005)

[27] T. Wejrzanowski, et al., Applied Surface Science 253, 204 (2006)

[28] R. Pielaszek, Analytical expression for diffraction line profile for polydispersive powders, Appl. Crystallography, Proceedings of the XIX Conference, Krakow, Poland, September, (2003) 43

[29] W. Wang, et al., Adv. Mater. 14, 837 (2002)

[30] N. Gupta, et al., J. Magn. Magn. Mater. 308, 137 (2007)

[31] E. Winkler, et al., Physical Review B 70, 174406 (2004)

[32] G.S. Alvarez et al., J. Am. Chem. Soc. 129(29), 9102 (2007)